

Constraining Evolution of Magnetic Field Strength in Dissipation Region of Two BL Lac Objects

Xu-Liang Fan¹, Da-Hai Yan^{2,3}, Qingwen Wu⁴ and Xu Chen⁵

¹ School of Mathematics, Physics and Statistics, Shanghai University of Engineering Science, Shanghai 201620, China; fanxl@sues.edu.cn

² Yunnan Observatories, Chinese Academy of Sciences, Kunming 650011, China

³ Key Laboratory for the Structure and Evolution of Celestial Objects, Chinese Academy of Sciences, Kunming 650011, China

⁴ School of Physics, Huazhong University of Science and Technology, Wuhan 430074, China

⁵ Shandong Provincial Key Laboratory of Optical Astronomy and Solar-Terrestrial Environment, Institute of Space Sciences, Shandong University, Weihai, 264209, China

Received 20xx month day; accepted 20xx month day

Abstract With the assumption that the optical variability timescale is dominated by the cooling time of the synchrotron process for BL Lac objects, we estimate time dependent magnetic field strength of the emission region for two BL Lac objects. The average magnetic field strengths are consistent with those estimated from core shift measurement and spectral energy distribution modelling. Variation of magnetic field strength in dissipation region is discovered. Variability of flux and magnetic field strength show no clear correlation, which indicates the variation of magnetic field is not the dominant reason of variability origin. The evolution of magnetic field strength can provide another approach to constrain the energy dissipation mechanism in jet.

Key words: BL Lacertae objects: general — BL Lacertae objects: individual (S5 0716+714, BL Lacertae) — galaxies: magnetic fields

1 INTRODUCTION

Magnetic field and magnetization (characterized by magnetization parameter σ) inside jets are important to understand acceleration and energy dissipation mechanisms of relativistic jets (Lyubarsky 2010; Sikora & Begelman 2013; Blandford et al. 2019). The flux variability of jet is also suggested to be related to magnetic reconnection process (Giannios 2013; Fan et al. 2018; Shukla & Mannheim 2020). The methods to constrain magnetic field structure in jet are usually based on the polarization measurements (Hovatta

pc-scale jet, magnetic field strength can be estimated from modelling of multi-wavelength spectral energy distribution (SED) (Zhang et al. 2014; Chen 2018) and core shift measurements (with equipartition assumption, Pushkarev et al. 2012; Zamaninasab et al. 2014 or without equipartition assumption, Zdziarski et al. 2015).

According to the results of core shift measurement and several theoretical arguments, magnetic field strength decreases along jet, with $B \propto r^{-1}$, where r is the distance between jet and the central engine (O’Sullivan & Gabuzda 2009; Blandford & Königl 1979; Chen & Zhang 2021). Based on this relation, magnetic field strength inside the dissipation region was suggested to constrain the location of emission region (Wu et al. 2018; Yan et al. 2018).

Similar with the electromagnetic radiation, the strength of magnetic field strength is also suggested as variable over time (e.g., Bonnoli et al. 2011; Thiersen et al. 2019; Polkas et al. 2021). The variation of magnetic field strength could also be one possible origin of flux variability of blazars (Paggi et al. 2011). The results of core shift measurements showed that magnetic field strength was variable during the flux flares, which was possibly related to the new jet component (Plavin et al. 2019). The direction of magnetic field in jet is also found to be variable (Hodge et al. 2018).

Similar to the method based on SED modelling, discovering variation of magnetic field strength from core shift measurement is based on the flux measurement (Plavin et al. 2019). However, the magnetic field strength estimated by these two methods can differ by a factor of 3 (Nalewajko et al. 2014). There was also suggestions that biases from core shift measurements can overestimate magnetic field strength in jet (Pashchenko et al. 2020). Thus there needs an independent method to estimate the magnetic field strength and its evolution inside the dissipation region. If the optical variability are mainly dominated by the cooling from synchrotron radiation, the lower limit of the magnetic field strength can be constrained with the variability timescale (Böttcher et al. 2003). In this paper, we constrain the optical variability timescale of two BL Lac objects (BL Lacs) with high sampling intra-day observations. Then we estimate the magnetic field strength of their emission regions and explore its evolution at timescales of years. In Section 2, we give the method to estimate magnetic field strength based on the optical photometric data, and the results of estimated variability timescale and magnetic field strength. Comparison of magnetic field strength with results derived from other methods and implications for evolution of magnetic field strength are discussed in Section 3. Section 4 summarizes the main conclusions.

2 METHOD AND RESULTS

The SEDs of blazars are dominated by the non-thermal radiation of jet, which show two bumps on the $\nu - \nu F_\nu$ diagram (Abdo et al. 2010). The low energy bump is believed to be produced by synchrotron emission. Synchrotron self-Compton (SSC) is suggested as the dominant mechanism for the high energy bump of BL Lacs — a subclasses of blazars with weak emission lines, especially high energy peaked BL Lacs (HBLs) (Abdo et al. 2010).

The intra-day or micro variability at optical band is a characteristic property of BL Lacs (Wagner & Witzel 1995). The timescale of the intra-day variability can be as short as several minutes (e.g., Bai et al.

synchrotron radiation, combined with possible host starlight for nearby sources. Thus, by ignoring cooling from inverse Compton scattering, the typical variability timescale can be seen as the upper limit of the cooling time of synchrotron radiation.

The cooling time of the synchrotron radiation can be estimated by (Tavecchio et al. 1998; Böttcher et al. 2003)

$$t_{cool} = \frac{3}{4} \frac{m_e c^2}{\sigma_T c} (\gamma u_B)^{-1} = \frac{6\pi m_e c}{\sigma_T \gamma B^2} \text{ s}, \quad (1)$$

where $u_B = B^2/8\pi$ is the energy density of the magnetic field, m_e is the mass of electron, σ_T is the cross section of Thomson scattering, γ is the electron energy. Meanwhile, the observational frequency is related to the electron energy γ with

$$\nu = \frac{4}{3} \nu_L \gamma^2 \frac{\delta}{1+z} = 3.7 \times 10^6 \gamma^2 B \frac{\delta}{1+z} \text{ Hz}, \quad (2)$$

where $\nu_L = 2.8 \times 10^6 B$ is the Larmor frequency, δ is the Doppler factor, and z is redshift.

Considering the observational variability timescale as the upper limit of t_{cool} , i.e., $t_{var} \delta / (1+z) \geq t_{cool}$, one can get the lower limit of the magnetic field strength combined equation 1 and 2,

$$B \geq 1.31 \times 10^8 t_{var}^{-2/3} \nu^{-1/3} \delta^{-1/3} (1+z)^{1/3} \text{ G}, \quad (3)$$

where t_{var} in unit of second and ν in unit of Hz. B is in unit of Gauss.

Based on Equation 3, if the observational variability timescale is obtained for a blazar, one can estimate the lower limit of the magnetic field strength with a special Doppler factor (taken as 10 throughout this paper). Our purpose in this work is to estimate the magnetic field strength with the intra-day variability timescale and explore its possible evolution. Therefore, we search the literature between 1990 and 2016 for the historical lightcurve at R band ($\nu = 4.6769 \times 10^{14}$ Hz). There are two sources (S5 0716+714 and BL Lacertae) with relatively more data and higher data sampling to derive the variability timescale on days or even hours (the references are list in Table 1). The lightcurves of both sources are shown in Figure 1. For both sources, the lightcurve is divided into intra-day timescales according to the observed time (Julian day). If the time interval of two adjacent data points is longer than two hours, we just divide them into two lightcurves. Otherwise they will be considered to belong to a single lightcurve. This criterion is for the relatively continuous lightcurve without large time gaps, and it will not divide the lightcurves across two Julian days. In order to estimate the variability timescale better, we intend to choose the intra-day lightcurves with relatively better sampling, longer lasting observed time, as well as obvious variability. Thus, the lightcurves with observed time spanning longer than 0.5 hour, number of data points larger than 20, and magnitude varying more than 5σ (where σ is the observational errors) are retained. Then the lightcurves are inspected by eyes to exclude the ones with random variations caused by the weather conditions or instrumental reasons. After these selection criteria, the number of intra-day lightcurves is significantly reduced. For the remaining lightcurves, we estimate the variability timescale of each lightcurve with (Wagner & Witzel 1995)

$$\tau = \frac{\langle F \rangle}{|\Delta F / \Delta t|} \quad (4)$$

where $\langle F \rangle$ is the average flux during the observational time range of individual lightcurve, ΔF is the flux difference between the maximum and minimum flux, Δt is the time between the maximum and minimum

Table 1: The references for historical data

Objects	Reference
S5 0716+714	Q02, R03, G06, M06, G08, Z08, P09, C11, B13, H14, D15, WEBT (V00, V08, O06)
BL Lac	B98, B99, X99, F00, F01, C01, H04, Z04, G06, WEBT (V09, R09, R10)
Notes: B98: Bai et al. (1998) , B99: Bai et al. (1999) , X99: Xie et al. (1999) , F00: Fan & Lin (2000) , V00: Villata et al. (2000) , C01: Clements & Carini (2001) , F01: Fan et al. (2001) , Q02: Qian et al. (2002) , R03: Raiteri et al. (2003) , H04: Hagen-Thorn et al. (2004) , Z04: Zhang et al. (2004) , G06: Gu et al. (2006) , M06: Montagni et al. (2006) , O06: Ostorero et al. (2006) , G08: Gupta et al. (2008) , V08: Villata et al. (2008) , Z08: Zhang et al. (2008) , P09: Poon et al. (2009) , R09: Raiteri et al. (2009) , V09: Villata et al. (2009) , R10: Raiteri et al. (2010) , C11: Chandra et al. (2011) , B13: Bhatta et al. (2013) , H14: Hu et al. (2014) , D15: Dai et al. (2015)	

The variability timescales range from $3.47 \times 10^4 s$ to $9.12 \times 10^5 s$ for S5 0716+714, and from $1.74 \times 10^4 s$ to $2.34 \times 10^5 s$ for BL Lacertae. Based on the variability timescales, we estimate the lower limit of the magnetic field strength for the selected time range with Equation 3 (z is taken as 0.3 and 0.0686 for S5 0716+714 and BL Lacertae, respectively). The variations of the magnetic field over time for both sources are plotted in Figure 1

The maximum magnetic field strengths for S5 0716+714 and BL Lacertae are $\log B = -0.09$ and 0.08, respectively, while the minimum ones are -1.05 and -0.68, respectively. The mean values and standard deviation of $\log B$ are -0.51 and 0.16 for S5 0716+714, which are -0.32 and 0.19 for BL Lacertae. Both S5 0716+714 and BL Lacertae show obvious variations on magnetic field strength ($\Delta B > 3\sigma_B$).

3 DISCUSSION

3.1 The strength of magnetic field inside emission region

There are several methods to estimate magnetic field strength in jet. The most widely used method for emission region of blazar is based on the SED modelling. [Anjum et al. \(2020\)](#) modelled the SED of these two sources with the quasi-simultaneous multi-frequency data. They derive $\log B = -0.33$ and -0.08 for S5 0716+714 and BL Lacertae, respectively. [Chen \(2018\)](#) also estimated the parameter of radiation for a sample of Fermi blazars with approximate analytical expressions. The magnetic field strengths $\log B = -1.05$ and 0.64 are derived for S5 0716+714 and BL Lacertae, respectively.

Core shift measurement provides another method to estimate magnetic field strength and electron number density in jet. The standard method assumes equipartition between the energy of magnetic field and particle, and estimates the magnetic field strength at 1 pc from jet vertex, which further infers the B strength of radio core with $B \propto r^{-1}$ ([O’Sullivan & Gabuzda 2009](#)). This method gives that $\log B_{1pc} = -0.31$ and -1.05 for S5 0716+714 and BL Lacertae, respectively ([Pushkarev et al. 2012](#)). For the 15 GHz core, $\log B = -1.15$ and -0.96 for S5 0716+714 and BL Lacertae, respectively ([Pushkarev et al. 2012](#)).

The deviation of magnetic fields strengths estimated from different methods above can be as large as 1.7 dex. [Nalewajko et al. \(2014\)](#) attempted to reconcile the magnetic dominated jet and the high Compton dominance for flat spectrum radio quasars (FSRQs), as well as the higher magnetic field strengths estimated from core shift measurements. They suggested inhomogeneous magnetic field structure in jet as a potential explanation. The emission region has lower local magnetic field strength compared to the overall jet, due

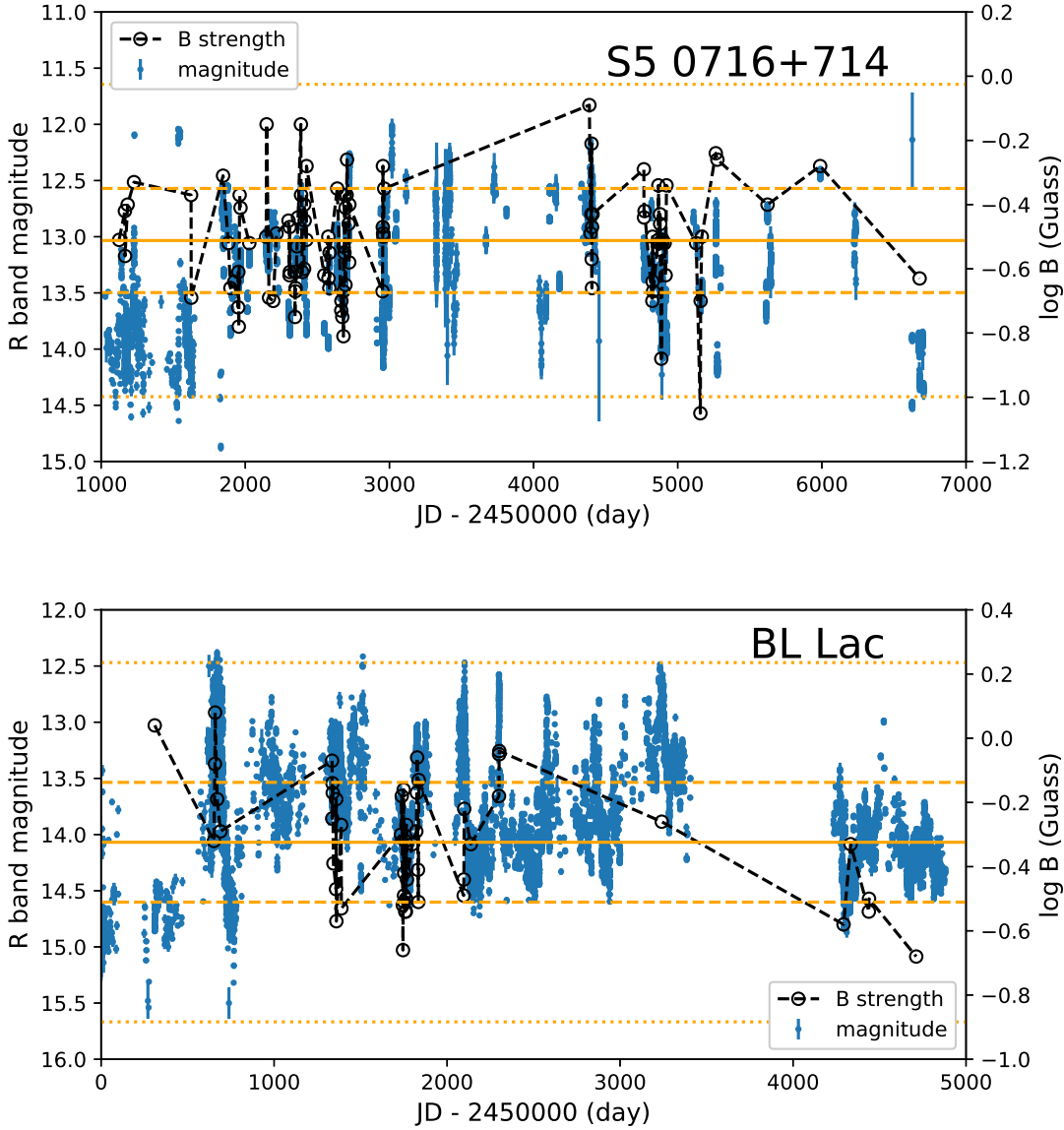


Fig. 1: The variations of lower limit of magnetic field strength and R band magnitude for S5 0716+714 (Upper panel) and BL Lacertae (Lower panel). The orange solid lines show the mean values of magnetic field strength. The dashed and dotted lines represent 1σ and 3σ for the distribution of $\log B$, respectively.

measurement are not always higher than that from SED modelling, e.g., 0.9 G given by [Pushkarev et al. \(2012\)](#) versus 1.56 G given by [Chen \(2018\)](#) for FSRQs. In Figure 2, all magnetic field strengths of S5 0716+714 and BL Lacertae listed above are plotted, as well as the mean values of those estimated from optical variability in this work. Generally, magnetic field strengths estimated by this work are at the middle of the other two methods. Considering the large uncertainty in various methods, the magnetic field strength estimated with optical variability is consistent with the results of other estimations.

In section 2, we estimate the lower limit of magnetic field strength with a certain value of Doppler factor (taken as 10). The value of $\log B$ would increase by 0.10 and decrease by 0.23 when the Doppler factor taken as 5 and 50, respectively. Even the most extreme values are considered, the estimated magnetic

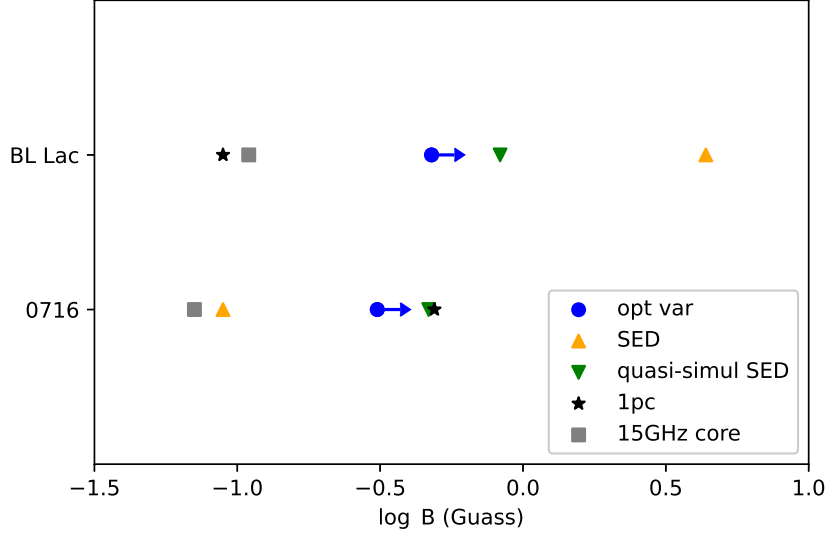


Fig. 2: Comparison of the estimated magnetic field strength with different methods. The blue circles with arrows represent the mean values of the lower limit of magnetic field strength estimated in this work. See the text for details.

variable along time. This scenario is suggested by [Raiteri et al. \(2017\)](#) to explain the long-term variability of blazars (also see [Raiteri et al. 2021](#)). The varied Doppler factors will result in varied observational variability timescale. Then the estimated magnetic field strength will also **vary** according to the variation of Doppler factor. Our results show no obvious long-term trend on the variation of magnetic field strength (Figure 1). However, the variation of estimated magnetic field strength is caused by variation of Doppler factor can not be excluded. More investigations and independent constraints for the variation of Doppler factor are needed in the future.

Magnetic field strength measurement is important to clarify the radiation mechanism of blazars, as strong magnetic field (about three orders of magnitude higher than that of leptonic model) is required for hadronic model, especially for proton synchrotron emission (e.g., [Hovatta & Lindfors 2019](#); [Cerruti 2020](#)). The magnetic field $\lesssim 1$ G estimated by all three methods above disfavors proton synchrotron emission for high energy emission, while leptonic or lepto-hadronic model can be compatible with it ([Cerruti 2020](#)).

[Yan et al. \(2018\)](#) proposed a method to locate the emission region with the estimation of magnetic field strength. If the magnetic field strength estimated from optical variability and core shift are both correct, combined with the relation $B \propto r^{-1}$, one can constrain the location of emission zone. This method requires a precondition that magnetic field strength and location of emission region should be stable along time. Once B strength in the emission region can be variable, simultaneous measurements are needed for the application of the relation of decreasing B strength with distance.

3.2 The evolution of magnetic field strength

As discussed above, under the assumption that the B strength is stable at special location in jet, the strength

of years, the observational evolution of B strength means the variation of emission region in jets. As the expectation of adiabatic expansion of jet, the blob would move outward from jet base, which results in decrease of B strength along time. No such continuous behaviours are found in Figure 1.

On the opposite, variable magnetic field along time can also cause the flux variability. Figure 1 shows the variation of magnetic field strength of two BL Lacs, as well as their flux variability. No clear trend is found between variability of flux and B strength. This indicates that variation of magnetic field strength in emission region is not the dominant reason of flux variability. The variability origin is not only related to the variation of magnetic field strength, but also other factors. The variation of magnetic field strength can be caused by new jet components as suggested by [Plavin et al. \(2019\)](#), or by turbulence components ([Marscher & Jorstad 2021](#)).

Polarization observation is an important tool to constrain structure of magnetic field in jet ([Hovatta & Lindfors 2019](#)). Intra-night variability of polarization degree and position angle was also found for S5 0716+714 and BL Lacertae ([Bhatta et al. 2016](#); [Weaver et al. 2020](#); [Marscher & Jorstad 2021](#)). The results of polarization behaviors indicated superposition of different turbulent regions or magnetic reconnection. [Marscher & Jorstad \(2021\)](#) demonstrated results of their multi-band flux and polarization monitoring for several blazars (including S5 0716+714 and BL Lacertae in this work). They compared the observed results with the predictions of Turbulent Extreme Multi-Zone model, and concluded that disordered magnetic field is important to produce the observed polarization behaviors. To distinguish different energy dissipation processes, combined the polarization variability with the variation of magnetic field strength before and after the flares could be useful. The magnetic field strength is expected to increase before and after shock regions, while it would decrease at the downstream of magnetic reconnection due to conversion from magnetic energy to kinetic energy of radiative particles (e.g., [Yamada et al. 2010](#); [Sironi et al. 2015](#)). Our method provide an approach to estimate magnetic field strength with continuous, high cadence optical observations.

4 CONCLUSIONS

In this paper, we estimate the optical variability timescale of two BL Lacs with high sampling intra-day lightcurve. Under the assumption that the cooling timescale is dominated by the synchrotron radiation for BL Lacs, we estimate the lower limit of magnetic field strength inside the emission zone. The similar results compared with other methods prove the validity of this method. More importantly, this method can constrain the evolution of magnetic field strength along time. Our results give an independent evidence that the magnetic field strength is variable in the dissipation region of jet. Works with better sampling data and combining polarization observations should give more constraints on the variability origin and energy dissipation mechanisms.

Acknowledgements We thank the anonymous referee for the useful comments. This work is supported by National Natural Science Foundation of China (NSFC; grant number 11803081, 11947099, U1931203, and 12003014). The work of D. H. Yan is also supported by the CAS Youth Innovation Promotion Association and Basic research Program of Yunnan Province (202001AW070013). Fractional of this work is based on data taken and assembled by the WEBT collaboration and stored in the WEBT archive at the Osservatorio

References

- Abdo, A. A., Ackermann, M., Agudo, I., et al. 2010, *ApJ*, 716, 30 [2](#)
- Anjum, M. S., Chen, L., & Gu, M. 2020, *ApJ*, 898, 48 [4](#)
- Bai, J. M., Xie, G. Z., Li, K. H., Zhang, X., & Liu, W. W. 1998, *A&AS*, 132, 83 [2, 4](#)
- Bai, J. M., Xie, G. Z., Li, K. H., Zhang, X., & Liu, W. W. 1999, *A&AS*, 136, 455 [4](#)
- Bhatta, G., Webb, J. R., Hollingsworth, H., et al. 2013, *A&A*, 558, A92 [4](#)
- Bhatta, G., Stawarz, Ł., Ostrowski, M., et al. 2016, *ApJ*, 831, 92 [7](#)
- Blandford, R. D., & Königl, A. 1979, *ApJ*, 232, 34 [2](#)
- Blandford, R., Meier, D., & Readhead, A. 2019, *ARA&A*, 57, 467 [1](#)
- Bonnoli, G., Ghisellini, G., Foschini, L., Tavecchio, F., & Ghirlanda, G. 2011, *MNRAS*, 410, 368 [2](#)
- Böttcher, M., Marscher, A. P., Ravasio, M., et al. 2003, *ApJ*, 596, 847 [2, 3](#)
- Cerruti, M. 2020, *Galaxies*, 8, 72 [6](#)
- Chandra, S., Baliyan, K. S., Ganesh, S., & Joshi, U. C. 2011, *ApJ*, 731, 118 [4](#)
- Chen, L. 2018, *ApJS*, 235, 39 [2, 4, 5](#)
- Chen, L., & Zhang, B. 2021, *ApJ*, 906, 105 [2](#)
- Clements, S. D., & Carini, M. T. 2001, *AJ*, 121, 90 [4](#)
- Dai, B.-z., Zeng, W., Jiang, Z.-j., et al. 2015, *ApJS*, 218, 18 [4](#)
- Fan, J. H., & Lin, R. G. 2000, *ApJ*, 537, 101 [4](#)
- Fan, J. H., Qian, B. C., & Tao, J. 2001, *A&A*, 369, 758 [4](#)
- Fan, J. H., Zhang, Y. W., Qian, B. C., et al. 2009, *ApJS*, 181, 466 [2](#)
- Fan, X.-L., Li, S.-K., Liao, N.-H., et al. 2018, *ApJ*, 856, 80 [1](#)
- Giannios, D. 2013, *MNRAS*, 431, 355 [1](#)
- Gu, M. F., Lee, C.-U., Pak, S., Yim, H. S., & Fletcher, A. B. 2006, *A&A*, 450, 39 [4](#)
- Gupta, A. C., Fan, J. H., Bai, J. M., & Wagner, S. J. 2008, *AJ*, 135, 1384 [4](#)
- Hagen-Thorn, V. A., Larionov, V. M., Larionova, E. G., et al. 2004, *Astronomy Letters*, 30, 209 [4](#)
- Hodge, M. A., Lister, M. L., Aller, M. F., et al. 2018, *ApJ*, 862, 151 [1, 2](#)
- Hovatta, T., & Lindfors, E. 2019, *New Astron. Rev.*, 87, 101541 [6, 7](#)
- Hovatta, T., Lister, M. L., Aller, M. F., et al. 2012, *AJ*, 144, 105 [1](#)
- Hu, S. M., Chen, X., Guo, D. F., Jiang, Y. G., & Li, K. 2014, *MNRAS*, 443, 2940 [2, 4](#)
- Lyubarsky, Y. E. 2010, *MNRAS*, 402, 353 [1](#)
- Marscher, A. P., & Jorstad, S. G. 2021, *Galaxies*, 9, 27 [7](#)
- Montagni, F., Maselli, A., Massaro, E., et al. 2006, *A&A*, 451, 435 [4](#)
- Nalewajko, K., Sikora, M., & Begelman, M. C. 2014, *ApJ*, 796, L5 [2, 4](#)
- Ostorero, L., Wagner, S. J., Gracia, J., et al. 2006, *A&A*, 451, 797 [4](#)
- O’Sullivan, S. P., & Gabuzda, D. C. 2009, *MNRAS*, 400, 26 [2, 4](#)
- Paggi, A., Cavaliere, A., Vittorini, V., D’Ammando, F., & Tavani, M. 2011, *ApJ*, 736, 128 [2](#)
- Pashchenko, I. N., Plavin, A. V., Kutkin, A. M., & Kovalev, Y. Y. 2020, *MNRAS*, 499, 4515 [2](#)
- Plavin, A. V., Kovalev, Y. Y., Pushkarev, A. B., & Lobanov, A. P. 2019, *MNRAS*, 485, 1822 [2, 7](#)
- Polkas, M., Petropoulou, M., Vasilopoulos, G., et al. 2021, *MNRAS*, 505, 6103 [2](#)

- Poon, H., Fan, J. H., & Fu, J. N. 2009, *ApJS*, 185, 511 [4](#)
- Pushkarev, A. B., Hovatta, T., Kovalev, Y. Y., et al. 2012, *A&A*, 545, A113 [2, 4, 5](#)
- Qian, B., Tao, J., & Fan, J. 2002, *AJ*, 123, 678 [4](#)
- Raiteri, C. M., Villata, M., Tosti, G., et al. 2003, *A&A*, 402, 151 [4](#)
- Raiteri, C. M., Villata, M., Capetti, A., et al. 2009, *A&A*, 507, 769 [4](#)
- Raiteri, C. M., Villata, M., Bruschini, L., et al. 2010, *A&A*, 524, A43 [4](#)
- Raiteri, C. M., Villata, M., Acosta-Pulido, J. A., et al. 2017, *Nature*, 552, 374 [6](#)
- Raiteri, C. M., Villata, M., Carosati, D., et al. 2021, *MNRAS*, 501, 1100 [6](#)
- Shukla, A., & Mannheim, K. 2020, *Nature Communications*, 11, 4176 [1](#)
- Sikora, M., & Begelman, M. C. 2013, *ApJ*, 764, L24 [1](#)
- Sironi, L., Petropoulou, M., & Giannios, D. 2015, *MNRAS*, 450, 183 [7](#)
- Tavecchio, F., Maraschi, L., & Ghisellini, G. 1998, *ApJ*, 509, 608 [3](#)
- Thiersen, H., Zacharias, M., & Böttcher, M. 2019, *Galaxies*, 7, 35 [2](#)
- Villata, M., Mattox, J. R., Massaro, E., et al. 2000, *A&A*, 363, 108 [4](#)
- Villata, M., Raiteri, C. M., Larionov, V. M., et al. 2008, *A&A*, 481, L79 [4](#)
- Villata, M., Raiteri, C. M., Larionov, V. M., et al. 2009, *A&A*, 501, 455 [4](#)
- Wagner, S. J., & Witzel, A. 1995, *ARA&A*, 33, 163 [2, 3](#)
- Weaver, Z. R., Williamson, K. E., Jorstad, S. G., et al. 2020, *ApJ*, 900, 137 [7](#)
- Wu, L., Wu, Q., Yan, D., Chen, L., & Fan, X. 2018, *ApJ*, 852, 45 [2](#)
- Xie, G. Z., Li, K. H., Zhang, X., Bai, J. M., & Liu, W. W. 1999, *ApJ*, 522, 846 [4](#)
- Yamada, M., Kulsrud, R., & Ji, H. 2010, *Reviews of Modern Physics*, 82, 603 [7](#)
- Yan, D., Wu, Q., Fan, X., Wang, J., & Zhang, L. 2018, *ApJ*, 859, 168 [2, 6](#)
- Zamaninasab, M., Clausen-Brown, E., Savolainen, T., & Tchekhovskoy, A. 2014, *Nature*, 510, 126 [2](#)
- Zdziarski, A. A., Sikora, M., Pjanka, P., & Tchekhovskoy, A. 2015, *MNRAS*, 451, 927 [2](#)
- Zhang, J., Sun, X.-N., Liang, E.-W., et al. 2014, *ApJ*, 788, 104 [2](#)
- Zhang, X., Zhang, L., Zhao, G., et al. 2004, *AJ*, 128, 1929 [4](#)
- Zhang, X., Zheng, Y. G., Zhang, H. J., et al. 2008, *AJ*, 136, 1846 [4](#)